Journal of Materials Chemistry

Cite this: J. Mater. Chem., 2012, 22, 14727

www.rsc.org/materials

PAPER

A counter electrode based on hollow spherical particles of polyaniline for a dye-sensitized solar cell†

Kuan-Chieh Huang,[a] Chih-Wei Hu,[a] Chen-Ya Tseng,[a] Chen-Yu Liu,[a] Min-Hsin Yeh,[a] Hung-Yu Wei,[b] Chun-Chieh Wang,[a] R. Vittal,[a] Chih-Wei Chu[cd] and Kuo-Chuan Ho*[ab]

Received 13th April 2012, Accepted 30th May 2012
DOI: 10.1039/c2jm32316h

Hollow spherical polyaniline (hsPANI) particles are synthesized and deposited on an ITO/glass substrate to prepare a counter electrode (designated as hsPANI-CE) for a dye-sensitized solar cell (DSSC). The structure and crystallization of the hsPANI particles are characterized by using high resolution transmission electron microscopy (HR-TEM), field-emission scanning electron microscopy (FE-SEM), X-ray diffractometry (XRD), X-ray photoelectron spectroscopy (XPS), and Raman spectra. A power-conversion efficiency (η) of 6.84% is obtained for the DSSC with the hsPANI-CE, while it is 6.02% in the case of the DSSC with a CE based on pristine PANI (designated as PANI-CE). Such enhancement is attributed to the hsPANI film having a larger active surface area (A) of 0.191 cm^2, compared to that of the PANI film (A = 0.126 cm^2), both values being estimated by a rotating disk electrode (RDE). Cyclic voltammetric (CV) curves have evidenced that the electro-catalytic ability of the hsPANI-CE for the reduction of tri-iodide (I_3^-) ions is higher than that of the PANI-CE. As a reference, the DSSC with a Pt-sputtered CE gives an η of 7.17%. Electrochemical impedance spectroscopic (EIS) spectra are used to substantiate the photovoltaic behaviors. The results suggest that the film consisting of hsPANI particles can be a potential catalytic layer for the replacement of Pt in the CE of a DSSC.

1. Introduction

A thin film of platinum (Pt) has been widely applied as the catalytic layer on the counter electrode (CE) of a DSSC, because of its outstanding electro-catalytic ability for the reduction of tri-iodide (I_3^-) in the electrolyte of the DSSC.[1–3] However, Pt is one of the most expensive components in a DSSC. Fabrication of CEs with other cheaper materials is expected to bring down the production cost of the cells, especially when it is a matter of large-scale production. Several materials, such as carbon materials,[4–6] conducting polymers,[7–9] TiN,[10] Mo_2N,[11] WO_2,[12] NbO_2,[13] CoS,[14] and NiS[15] have been investigated as alternatives to replace Pt for the CE of a DSSC. Among various conducting polymers, polyaniline (PANI) has been studied most intensively due to its exceptional electrical, catalytic, and electrochemical properties.[16] On account of its high environmental stability and owing to the low cost of aniline (ANI) monomers, PANI stimulates several investigations for the fabrication of efficient electronic devices.[17,18] Poly(3,4-ethylenedioxythiophene) (PEDOT) was the first conducting polymer used as the catalyst for the CE of a DSSC.[19] Recently, a few attempts have been made to replace Pt with PANI as the catalytic layer for the CE of a DSSC, intending to reduce the cost of production of the DSSCs.[8,20–22] Even though pristine PANI is good enough to be utilized for a CE, its relatively low electro-catalytic ability still limits the power-conversion efficiency (η) of its DSSC. Tran *et al.* have reported that several nanostructures of PANI can be synthesized *via* the oxidation of ANI monomers.[23] Studies have also been carried out on the preparation of nanostructures of PANI with hollow spheres.[24,25]

In this study, we report the synthesis of hollow spherical polyaniline (hsPANI) particles, their deposition on the CE of a DSSC. The η of 6.84% of the cell with hsPANI particles is found to be close to that of the cell with a Pt-coated CE (η = 7.17%), under illumination of 1 sun. To the best of our knowledge, this is the first study to report the performance of a DSSC with a CE consisting of a catalytic layer of hollow spherical particles of PANI. High resolution transmission electron microscopic (HR-TEM) pictures are shown for a hsPANI particle at various rotating angles. Especially, a detailed

[a]Department of Chemical Engineering, National Taiwan University, Taipei 10617, Taiwan. E-mail: kcho@ntu.edu.tw; Fax: +886-2-2362-3040; Tel: +886-2-2366-0739
[b]Institute of Polymer Science and Engineering, National Taiwan University, Taipei 10617, Taiwan
[c]Research Center for Applied Sciences, Academia Sinica, Taipei 11529, Taiwan
[d]Department of Photonics, National Chiao Tung University, Hsinchu 300, Taiwan

† Electronic supplementary information (ESI) available. See DOI: 10.1039/c2jm32316h

description is made of the estimation of the active electro-catalytic surface areas of the films of PANI and hsPANI, based on the rotating disk electrode (RDE) technique.

2. Experimental

2.1. Materials

ANI monomer, anhydrous LiI, I_2, acetonitrile (AN), and poly(ethylene glycol) (PEG, $M_w = 20\,000$) were purchased from Merck. Ammonium persulfate (APS) was received from J. T. Baker. Lithium perchlorate ($LiClO_4$), β-naphthalene sulfonic acid (NSA), tetrabutylammonium triiodide ($TBAI_3$, >97%), hydrochloric acid (HCl, 37%), and nitric acid (HNO_3, 65%) were obtained from Sigma-Aldrich. Titanium(IV) isopropoxide (TTIP, +98%), 4-*tert*-butylpyridine (TBP, 96%), and *tert*-butanol (*t*BuOH, 99.5%) were acquired from Acros. 3-methoxypropionitrile (MPN, 99%) was obtained from Fluka. *cis*-Bis(isothiocyanato)bis(2,2′-bipyridyl-4,4′-dicarboxylato)ruthenium(II)bis-tetrabutylammonium (N719) and 1,2-dimethyl-3-propylimidazolium iodide (DMPII) were purchased from Solaronix S. A., Aubonne, Switzerland.

2.2. Preparation of hollow spherical polyaniline (hsPANI) particles

The hsPANI particles were synthesized *via* a process of emulsion, in accordance with a previous report.[24] In brief, a 0.1 M aqueous solution of ANI monomers was first prepared. An amount of NSA was added to the ANI solution, so that its concentration was 2.3 mM in the final solution. This addition led to the formation of the ANI droplet with a core–shell structure; it was further analyzed that the droplet consisted of NSA/anilinium salt as the shell and ANI as the core. Subsequently, 10.0 mM of APS was then incorporated into the obtained solution at −10 °C for 48 h; this led to an *in situ* polymerization of the anilinium to PANI at the shell of the ANI droplets (Fig. 1).

2.3. Preparation of electrode with the film of pristine PANI and hollow spherical PANI

A thin film, containing pristine PANI and hsPANI, was deposited by electro-polymerization on an ITO/glass substrate as follows. The synthesized hsPANI particles were added into an ANI solution to a final concentration of 1.0 wt%, and then the contents were subjected to a process of reflux-condensation at 210 °C for 3 h. This solution was filtrated through a MF-Millipore mixed cellulose ester membrane (0.45 μm, Millipore). Filtered particles of hsPANI attached with ANI (hsPANI/ANI) were obtained. After the process of reflux-condensation at 210 °C for 3 h, the outer and inner surfaces of hsPANI particles were supposed to have been attached with ANI. This is confirmed because of the appearance of a characteristic absorption peak at around 280 nm,[26] corresponding to the absorption of pristine ANI in hsPANI/ANI. Also, the absorption peak at 400 to 430 nm corresponding to the green protonated PANI form[27] is observed (Fig. S1 in the ESI†). The inner surface of hsPANI was supposed to have been attached with ANI, based on the fact that the film of hsPANI has some opened spheres, that is to say that these open spheres could have allowed the entry of ANI into them. The attached ANI monomers of hsPANI/ANI particles were supposed to have been electrochemically polymerized to form PANI; thus the final film on the ITO/glass substrate is suggested to be a film containing pristine PANI and hsPANI particles. This ITO/glass substrate with the film of PANI and hsPANI was used as the counter electrode for a DSSC.

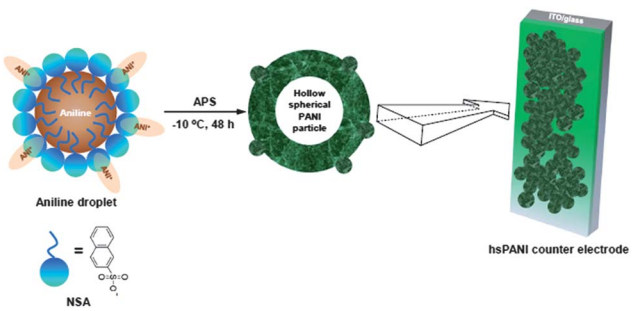

Fig. 1 Flowchart for the preparation of the hsPANI counter electrode.

ITO/glass (surface resistance = 10 Ω sq.$^{-1}$, Uni-Onward Corp., Taipei, Taiwan), Pt foil, and Ag/AgCl/saturated KCl were used as the working, auxiliary, and the reference electrodes, respectively in a three-electrode electrochemical system for the deposition of the film of hsPANI. An Autolab potentiostat/galvanostat (Eco Chemie, model PGSTAT30) was used for the deposition of the film of hsPANI onto the ITO/glass.

The film was deposited from an aqueous solution, consisting of 9.3 wt% of the refluxed hsPANI/ANI and 2.0 M of HCl, at an optimal charge capacity of 70 mC cm^{-2} by applying a constant potential of 0.8 V (*vs.* Ag/AgCl/saturated KCl). The electro-polymerization was stopped when the desired amount of charge was passed. The as-prepared ITO/glass with the film of hsPANI was rinsed with HCl solution and dried under air. Thus, an ITO/glass substrate with a thin film, consisting of hsPANI and PANI was finally obtained and used as the CE of a DSSC. A thin film of pristine PANI was also deposited on an ITO/glass substrate in another solution containing 1.0 M ANI and 2.0 M HCl by using the same electro-polymerizing setup, however, with an optimal depositing charge capacity of 50 mC cm^{-2}.

2.4. Preparation of the TiO_2 photoanode and assembly of the DSSC

TTIP was hydrolyzed to obtain TiO_2 in a medium containing HNO_3, by adopting a sol–gel method. Afterwards, the TiO_2 solution was autoclaved through a hydrothermal process at 240 °C for 12 h. By concentrating the autoclaved solution to 13 wt%, a paste of nanocrystalline TiO_2 was obtained. Then, 30 wt% of PEG with respect to TiO_2 was incorporated into the paste, intending to enhance the necking ability and to control the porosity of TiO_2. The thus obtained TiO_2 paste was deposited on an FTO/glass substrate (surface resistance = 7 Ω sq.$^{-1}$, TEC-7, Hartford Glass Co., Inc., Hartford City, Indiana, USA) by doctor-blade. The TiO_2-coated FTO/glass was annealed at 450 °C for 30 min. The active area of TiO_2 was controlled to be 0.16 cm^2. The TiO_2-coated FTO/glass was finally immersed in an AN/*t*BuOH (v/v = 1/1) solution containing 0.3 mM N719 for 12 h to obtain the photoanode for the DSSC. The DSSC was

assembled with the photoanode and the CE (hsPANI-CE or PANI-CE or Pt-CE) by keeping a distance of 25 μm between them by using Surlyn® (Solaronix) as the spacer, and by injecting the electrolyte, containing 0.6 M DMPII, 0.1 M LiI, 0.05 M I_2, and 0.5 M TBP in MPN, between the electrodes through a hole in the CE by a capillary method.

2.5. Instrumentation

HR-TEM images were obtained by using a Philip Tecnai G^2 LaB6 Gun Transmission Electron Microscope with Gatan Dual Vision CCD Camera, operated at 200 keV. Plane view images of the CEs were obtained by field-emission scanning electron microscopy (FE-SEM, Zeiss EM 902A). Cross-sectional images of the CEs were acquired using a SEM model of Nova™ NanoSEM 230. An X-ray diffractometer (XRD, X'Pert, Philips) was used to verify the crystallization of hsPANI particles. X-ray photoelectron spectroscopy (XPS) was accomplished by using a PHI 5000 Versaprobe ULVAC-PHI, and the background pressure in the analysis chamber was controlled at 10^{-5} Pa. Raman spectra were recorded by a Dimension-P2 Raman system (Lamba Solution, Inc.). A UV/VIS/NIR spectrophotometer (V-570, Jasco) was used to obtain the UV/Vis absorption spectra of the samples. The surface of the DSSC was illuminated by a class A quality solar simulator (PEC-L11, AM 1.5G, Peccell Technologies, Inc.) and the incident light intensity (1 sun, 100 mW cm^{-2}) was calibrated with a standard Si cell (PECSI01, Peccell Technologies, Inc.). The photocurrent density–voltage (J–V) curves and the electrochemical impedance spectroscopic (EIS) spectra of the DSSCs were recorded by a potentiostat/galvanostat (PGSTAT 30, Autolab, Eco-Chemie, the Netherlands). The electro-catalytic abilities of the CEs for the I^-/I_3^- redox process were analyzed by using cyclic voltammetry (CV), using a three-electrode system (PGSTAT 30, Autolab, Eco-Chemie, the Netherlands), in a conventional electrolyte, consisting of 10.0 mM LiI, 1.0 mM I_2, and 0.1 M $LiClO_4$ in AN, at a scan rate of 50 mV s^{-1}.

2.6. Electrochemical experiments with the rotating disk electrode (RDE)

A RDE based on a glassy carbon electrode (Part # AFE7R9GCGC, PINE Instrument Company) was deposited with a thin film of hsPANI or PANI by electro-polymerization, performed in the same way as that for the preparation of hsPANI-CE or PANI-CE. This RDE coated with the film of hsPANI or PANI had served as the working electrode, and a Pt wire and an Ag/Ag^+ electrode were employed as the auxiliary electrode and the reference electrode, respectively. The RDE system was equipped with a modulated speed rotator (MSR, PINE Instrument Company) and was connected to a potentiostat (model 900B, CH Instruments). The electrolyte used was an AN-based solution containing 0.1 M $LiClO_4$ and 1.0 mM $TBAI_3$. All potentials reported were referred to the reference electrode of Ag/Ag^+. CV curves were obtained by scanning the potential of the electrode from −0.8 to 1.0 V at a scan rate of 50 mV s^{-1} (in absence of rotation). The half-wave potential ($E_{1/2}$) of the redox couple of I_3^-/I^- was derived from the CV curve (not shown) of the RDE, which was coated with a thin film of hsPANI. Five linear sweep voltammetric (LSV) curves (not shown) were acquired for the film of hsPANI in the above-mentioned electrolyte, by controlling the MSR at various rotating speeds (50, 100, 200, 400, and 800 rpm), and by scanning the potential of the RDE from −0.7 to 0.2 V, at a scan rate of 1.0 mV s^{-1}; a corresponding current, i, could be obtained from each of the LSV curves at $E_{1/2}$. Thus, a plot of i^{-1} *vs.* $\omega^{-1/2}$ was made for the film of hsPANI. In the same way, the plot of i^{-1} *vs.* $\omega^{-1/2}$ was obtained for the pristine PANI film.

3. Results and discussion

3.1. Characterization of hollow spherical polyaniline (hsPANI) particles

Our HR-TEM results have shown a final product of hsPANI particles, indicating the escape of core ANI through the shells during the last process. HR-TEM images of an hsPANI particle are shown in Fig. 2a–d, in which the images were especially obtained at various rotating angles (0°, 20°, 40°, and 60°) of the sample holder. The lattice of the hsPANI particle was observed at its shell (Fig. 2e), but not at the amorphous core of the particle.

The d-spacing of this lattice through XRD measurement was about 3.5 Å at 2θ of 25.4° (Fig. 3a). The component of PANI in the hsPANI particle could be verified from the signal of N_{1s} at around 400 eV in the XPS full-scan spectrum (inset of Fig. 3a). The crystalline nature of the hsPANI particles was also verified by using selected area electron diffraction (SAED) mode of the HR-TEM (inset of Fig. 2e). Fig. 2f shows a large number of hsPANI particles; the hollow nature of the particles is indicated by the cracks in some of the particles. Furthermore, the inset of Fig. 2f shows some of the hsPANI particles with open structures. HR-TEM images thus demonstrate that particles of hsPANI consist of PANI in their shells. In Fig. 3b, Raman spectra of the particles of hsPANI and PANI show that they have the same characteristic peaks at 1386 and 1567 cm^{-1}; this clearly suggests

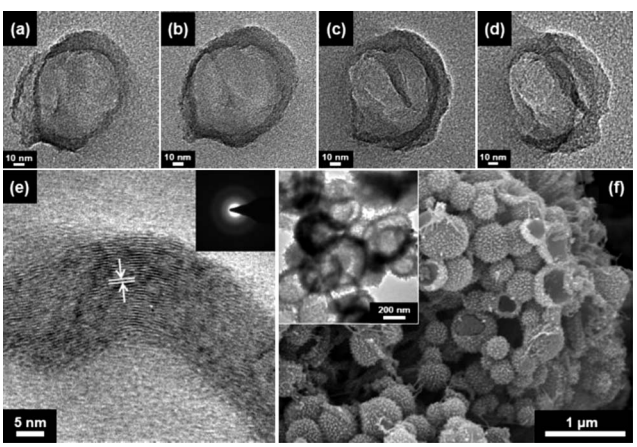

Fig. 2 HR-TEM images of a hsPANI particle, obtained at various rotating angles of the sample holder: (a) 0°, (b) 20°, (c) 40°, and (d) 60°. (e) Magnified version of (a). The inset of (e) shows the SAED image of the particle. (f) Plane view SEM image of the hsPANI particles; the inset of (f) shows the TEM image of the hsPANI particles having open structures.

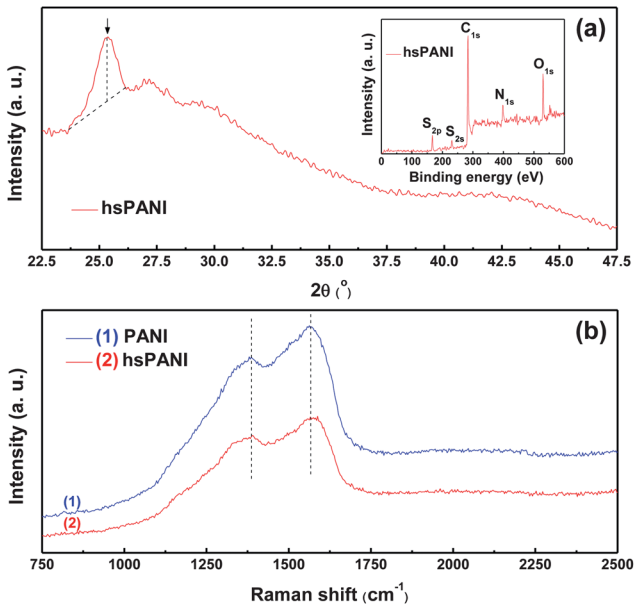

Fig. 3 (a) XRD pattern of hsPANI particles; inset of (a) shows a full-scan spectrum of XPS for hsPANI particles. (b) Raman spectra of pristine PANI and hsPANI particles.

that the inherent property of PANI is not disturbed in the hsPANI particles.

3.2. Surface morphologies of various thin films

Fig. 4a shows the plane view SEM image of the film of hsPANI. The film consists of a three dimensional network of hsPANI spheres. On the other hand, a rod-like configuration of the PANI film is exhibited in Fig. 4b. In comparison, another film of sputtering Pt was also deposited on an ITO/glass substrate using a Cressington 108 auto Sputter Coater (Cressington Scientific Instruments Ltd., Watford, UK) at 40 mA for 130 s. The Pt-sputtered film presents a relatively uniform and smooth surface morphology (Fig. 4c), as compared with the surface morphologies of films of hsPANI and PANI.

3.3. Photovoltaic performances and EIS spectra of the DSSCs with various counter electrodes

The J–V curves and the EIS spectra of the DSSCs with the CEs containing the films of hsPANI, PANI, and Pt, obtained at 100 mW cm^{-2} illumination are shown in Fig. 5a and b, respectively. The photovoltaic parameters and the interfacial charge-transfer resistance, R_{ct1}, are given in Table 1, where R_{ct1} represents the resistance at the interface between the CE and the electrolyte of a DSSC. The short-circuit current density (J_{SC}) and the open-circuit voltage (V_{OC}) of the DSSC using the CE coated with the film of hsPANI (designated as hsPANI-CE) are 16.26 mA cm^{-2} and 695 mV, respectively; the same parameters are 14.93 mA cm^{-2} and 668 mV for the DSSC applying the CE coated with the pristine PANI film (designated as PANI-CE). As the cells are the same except for the CEs, these enhancements suggest that the hsPANI-CE has a better electro-catalytic ability for the reduction of I_3^-, compared to the PANI-CE; this better electro-catalytic ability is established at a later stage through CV.

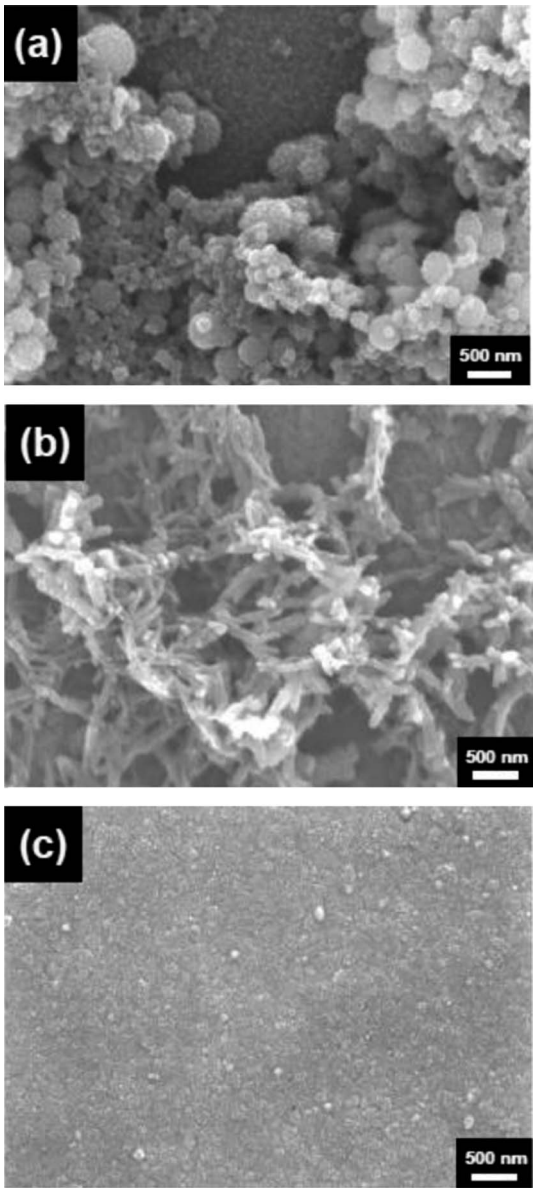

Fig. 4 Plane view SEM images of the films of (a) hsPANI, (b) PANI, and (c) Pt.

The better electro-catalytic ability of hsPANI-CE is in consistency with the smaller value of R_{ct1} for its DSSC ($R_{ct1} = 8.85\ \Omega$), compared to the value of R_{ct1} of the cell with the PANI-CE ($R_{ct1} = 9.13\ \Omega$). Thus, the DSSC with the hsPANI-CE delivered a higher η of 6.84% in comparison to that of the cell with the PANI-CE ($\eta = 6.02\%$). The η of the DSSC employing the hsPANI-CE is close to that of the cell with the Pt-CE ($\eta = 7.17\%$), which has an intrinsic property of extraordinary electro-catalytic ability (Table 1).

3.4. Analyses of electro-catalytic abilities of hsPANI and PANI films by RDE and CV

The remarkable electro-catalytic ability of hsPANI film is apparently due to its structure with partially hollow spherical particles, which could provide a high porosity and a large surface area to the film. To verify this, we have estimated the active

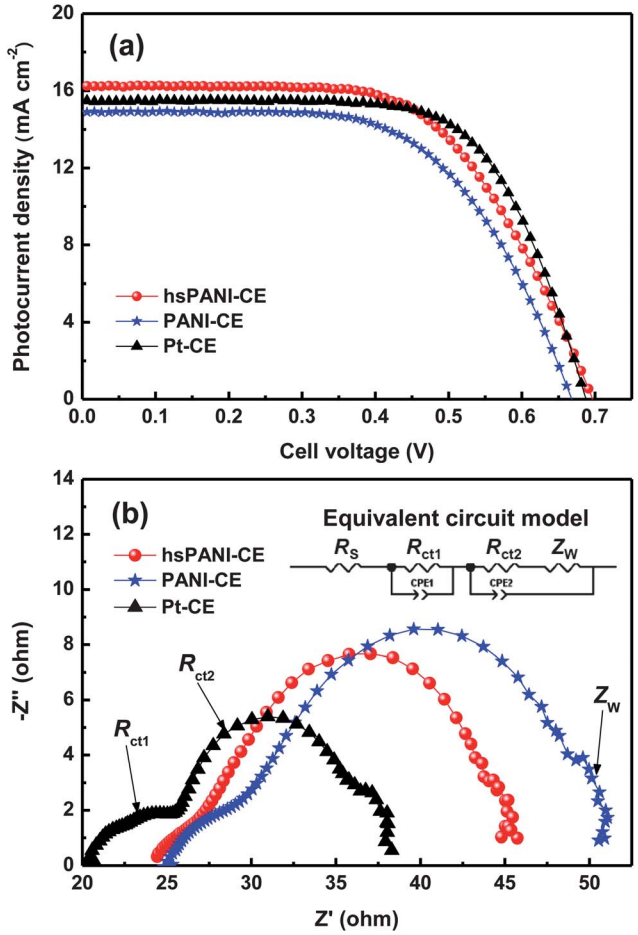

Fig. 5 (a) *J–V* curves and (b) EIS spectra of the DSSCs with the CEs containing the films of hsPANI, PANI, and Pt, obtained at 1 sun. The inset of (b) shows the corresponding equivalent circuit model.

Table 1 Photovoltaic parameters and R_{ct1} values of the DSSCs with hsPANI-CE, PANI-CE, and Pt-CE at an illumination of 100 mW cm^{-2}

CEs	V_{OC} (mV)	J_{SC} (mA cm^{-2})	FF	η (%)	R_{ct1} (Ω)
hsPANI-CE	695	16.26	0.61	6.84	8.85
PANI-CE	668	14.93	0.60	6.02	9.13
Pt-CE	689	15.47	0.67	7.17	8.33

surface areas (A) of both hsPANI-CE and PANI-CE by using an RDE. An RDE measurement is considered to obtain a very precise value of A for a porous nanostructured material. In brief, CV curves of thin films of hsPANI and PANI were obtained in an AN-based electrolyte, containing 0.1 M $LiClO_4$ and 1.0 mM $TBAI_3$, at a scan rate of 50 mV s^{-1}. The RDE was operated at various rotating speeds of 50, 100, 200, 400, and 800 rpm, and a scan rate of 1.0 mV s^{-1} was applied to obtain linear sweep voltammetric (LSV) curves for both hsPANI and PANI. The values of A were extracted by using the Koutecký–Levich equation, which relates the current to the rotating speed; the equation can be written as follows:[28]

$$\frac{1}{i} = \frac{1}{nFAkC} + \frac{1}{0.62nFAD^{2/3}\nu^{-1/6}\omega^{1/2}C} \quad (1)$$

where i is the limiting current, n of 2 is the number of electrons involved in the reaction, F is the Faraday constant, A is the active surface area, k is the rate constant, C of 1.0 mM is the concentration of I_3^-, D of 3.62×10^{-6} cm^2 s^{-1} is the diffusion coefficient of I_3^-, ν of 4.71×10^{-3} cm^2 s^{-1} is the kinematic viscosity of AN, and ω is the angular velocity converted from the rotating speed.

Fig. 6a shows the plots of i^{-1} *vs.* $\omega^{-1/2}$ for the films of hsPANI and PANI. The inset in Fig. 6a shows the porosity of the particles of hollow spherical PANI and spherical PANI. The values of A and k were calculated for the films of hsPANI and PANI from the slope and the intercept of Y-axis, respectively, using the Koutecký–Levich equation, after fitting the data in the plots for the two conditions. The results have evidenced that the structure of hollow spherical particles for the film of hsPANI has rendered a larger active surface area for it ($A = 0.191$ cm^2) than that of the film of PANI ($A = 0.126$ cm^2), which has a rod-like structure (see Fig. 4b). This higher A of the film of hsPANI is consistent with its inherent porous structure of hsPANI particles with a higher porosity of 73.5% (inset of Fig. 6a) than that of spherical PANI particles without hollow portions in them (56.3%); the porosity of

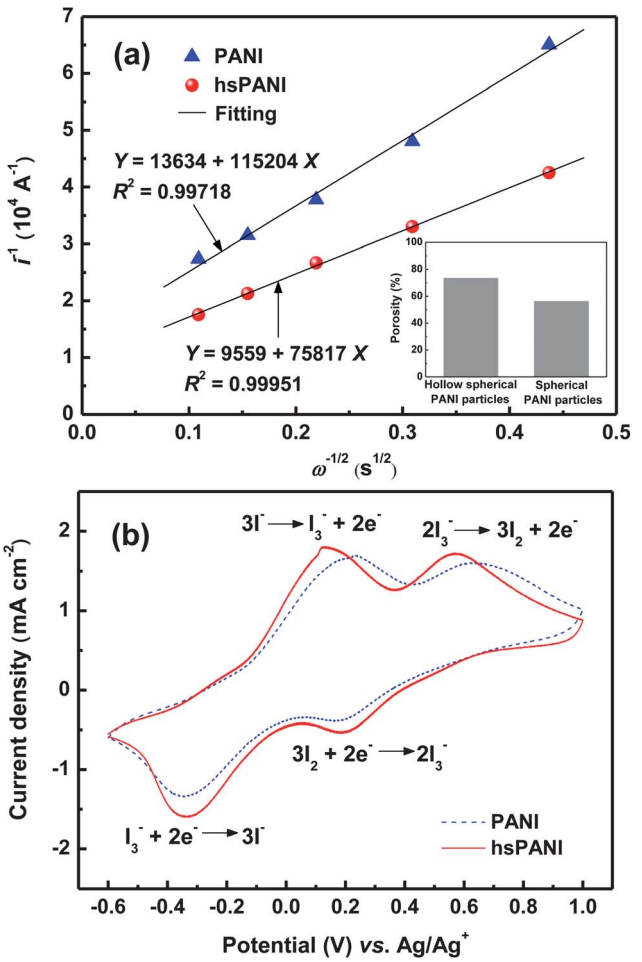

Fig. 6 (a) Plots of i^{-1} *vs.* $\omega^{-1/2}$ for the films of hsPANI and PANI. The inset shows the porosity of the particles of hollow spherical PANI and spherical PANI. (b) CV curves of the hsPANI-CE and the PANI-CE at a scan rate of 50 mV s^{-1}.

the particles was measured by a mercury porosimeter (Micromeritics, Autopore 9250). The spherical PANI particles were prepared in the same way as that used for the preparation of hsPANI particles, but without using NSA during the preparation process. The kinetic parameter, k, can be considered as the heterogeneous interfacial reacting rate at the interface between the CE and the electrolyte. Thus, the close values of k for films of hsPANI ($k = 2.9 \times 10^{-3}$ cm s^{-1}) and PANI ($k = 3.0 \times 10^{-3}$ cm s^{-1}) are due to the intrinsic property of the same material, PANI, in them.

The conductivities of hsPANI-CE and PANI-CE were evaluated using EIS in the frequency range of 65 kHz to 0.01 Hz (Fig. S2 in the ESI†). In brief, two identical CEs of hsPANI-CE or PANI-CE were separated by a Surlyn® in a symmetric cell. The space between the electrodes was filled with the same electrolyte as that used in a DSSC. In the EIS spectrum, the intercept of the X-axis obtained at the high frequency is the series resistance (R_s) of the symmetric cell. The R_s value is related to the inverse of conductivity of the symmetric cell and can be obtained by fitting the data using a relevant equivalent circuit model. The conductivity of PANI-CE ($R_s = 10.84\ \Omega$) was found to be slightly higher than that of hsPANI-CE ($R_s = 11.38\ \Omega$) (Fig. S2 in the ESI†). The higher conductivity of PANI-CE may be due to the rod-like configuration of the PANI film (see Fig. 4b), which can favor the transfer of electrons in a better way than in the case of the film of hsPANI, owing to a three dimensional network of hsPANI spheres. The boundaries between the spherical particles of hsPANI (see Fig. 4a) may retard the transfer of electrons, thereby lowering the conductivity of the film.

In Fig. 6b, each CV curve shows two pairs of peaks, corresponding to the electrochemical reactions as follows:[29]

$$I_3^- + 2e^- \leftrightarrow 3I^- \quad (2)$$

$$3I_2 + 2e^- \leftrightarrow 2I_3^- \quad (3)$$

The magnitude of the cathodic peak current density (i_{pc}) at around −0.4 to −0.3 V (*vs.* Ag/Ag$^+$) can be regarded as the electro-catalytic ability of the CE for the reduction of I_3^-. Thus, the electro-catalytic ability of the hsPANI-CE is higher than that of the PANI-CE. We have observed above that the conductivity of PANI film is better than that of hsPANI film. However, the surface area of hsPANI film is higher than that of PANI film, as measured by RDE. The performance of the counter electrode of a DSSC depends both on the conductivity and surface area of the catalytic film on it. Due to higher surface area, more active sites can be available on the film of hsPANI for the reduction of I_3^-, and thereby the electro-catalytic ability of its counter electrode can be higher. Due to better conductivity of the film of PANI, the transfer of electrons can be faster at its electrode and thereby the reduction of I_3^- can also be faster, which also favors a good electro-catalytic ability for its counter electrode. Since hsPANI shows higher electro-catalytic ability than PANI (see Fig. 6b), the overall positive effect appears to be due to surface area rather than conductivity, in the present case. The higher electro-catalytic ability of hsPANI-CE rendered a better performance for its DSSC ($\eta = 6.84\%$) than that of the cell with the PANI-CE ($\eta = 6.02\%$) (see Table 1).

The cross-sectional SEM pictures for the hsPANI-CE and the PANI-CE are shown in Fig. 7a and b, respectively. Since the thickness of the film of hsPANI ($(1.06 \pm 0.08) \times 10^{-4}$ cm) is close to that of the film of PANI ($(0.94 \pm 0.13) \times 10^{-4}$ cm), we believe that the difference in their A is essentially due to their morphological differences.

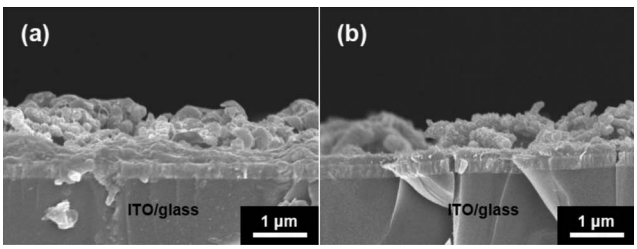

Fig. 7 Cross-sectional views of SEM images for the films of (a) hsPANI-CE and (b) PANI-CE.

4. Conclusions

In conclusion, we have obtained a thin film of hsPANI particles on an ITO/glass substrate in two steps, first by synthesizing the hsPANI particles *via* a process of emulsion and then by depositing the hsPANI particles on the ITO/glass substrate. The film consists of a three dimensional network of hsPANI spheres. Some of the hsPANI particles were found to contain open structures. The ITO/glass substrate with the film of hsPANI was used as the CE of a DSSC. The electro-catalytic ability of the hsPANI-CE is found to be higher than that of the PANI-CE. The better electro-catalytic ability of the hsPANI-CE is consistent with the smaller value of R_{ct1} for its DSSC, compared to the value of R_{ct1} of the cell with the PANI-CE. Electrochemical studies, by using a RDE, suggest that the CE with the film of hsPANI has a larger surface area, compared to that of the CE with the pristine PANI film. Thus, the DSSC with the hsPANI-CE delivered a higher η of 6.84% in comparison to that of the cell using the PANI-CE ($\eta = 6.02\%$). The η of the DSSC employing the hsPANI-CE is close to that of the cell with the Pt-CE ($\eta = 7.17\%$). Thus, the thin film consisting of hsPANI particles can serve as a potential catalytic layer to replace the expensive Pt layer for the CE of a DSSC.

Acknowledgements

We acknowledge the financial support received from the National Science Council (NSC) and Academia Sinica, Taiwan.

Notes and references

1 B. O'Regan and M. Grätzel, *Nature*, 1991, **353**, 737.
2 M. Grätzel, *J. Photochem. Photobiol., A*, 2004, **164**, 3.
3 N. Papageorgiou, *Coord. Chem. Rev.*, 2004, **248**, 1421.
4 S. I. Cha, B. K. Koo, S. H. Seo and D. Y. Lee, *J. Mater. Chem.*, 2010, **20**, 659.
5 H. Choi, H. Kim, S. Hwang, Y. Han and M. Jeon, *J. Mater. Chem.*, 2011, **21**, 7548.
6 L. Kavan, J. H. Yum and M. Grätzel, *Nano Lett.*, 2011, **11**, 5501.
7 J. M. Pringle, V. Armel and D. R. MacFarlane, *Chem. Commun.*, 2010, **46**, 5367.
8 Q. Tai, B. Chen, F. Guo, S. Xu, H. Hu, B. Sebo and X. Z. Zhao, *ACS Nano*, 2011, **5**, 3795.

9 S. S. Jeon, C. Kim, J. Ko and S. S. Im, *J. Mater. Chem.*, 2011, **21**, 8146.
10 G. R. Li, F. Wang, Q. W. Jiang, X. P. Gao and P. W. Shen, *Angew. Chem., Int. Ed.*, 2010, **49**, 3653.
11 M. Wu, Q. Zhang, J. Xiao, C. Ma, X. Lin, C. Miao, Y. He, Y. Gao, A. Hagfeldt and T. Ma, *J. Mater. Chem.*, 2011, **21**, 10761.
12 M. Wu, X. Lin, A. Hagfeldt and T. Ma, *Chem. Commun.*, 2011, **47**, 4535.
13 X. Lin, M. Wu, Y. Wang, A. Hagfeldt and T. Ma, *Chem. Commun.*, 2011, **47**, 11489.
14 M. K. Wang, A. M. Anghel, B. Marsang, N. L. C. La, N. Pootrakulchote, S. M. Zakeeruddin and M. Grätzel, *J. Am. Chem. Soc.*, 2009, **131**, 15976.
15 H. Sun, D. Qin, S. Huang, X. Guo, D. Li, Y. Luo and Q. Meng, *Energy Environ. Sci.*, 2011, **4**, 2630.
16 J. X. Huang, *Pure Appl. Chem.*, 2006, **78**, 15.
17 T. W. Lee, Y. Byun, B. W. Koo, I. N. Kang, Y. Y. Lyu, C. H. Lee, L. Pu and S. Y. Lee, *Adv. Mater.*, 2005, **17**, 2180.
18 M. Li, Y. Guo, Y. Wei, A. G. MacDiarmid and P. I. Lelkes, *Biomaterials*, 2006, **27**, 2705.
19 Y. Saito, T. Kitamura, Y. Wada and S. Yanagida, *Chem. Lett.*, 2002, **31**, 1060.
20 S. Ameen, M. S. Akhtar, Y. S. Kim, O. B. Yang and H. S. Shin, *J. Phys. Chem. C*, 2010, **114**, 4760.
21 Z. Li, B. Ye, X. Hu, X. Ma, X. Zhang and Y. Deng, *Electrochem. Commun.*, 2009, **11**, 1768.
22 Q. H. Li, J. H. Wu, Q. W. Tang, Z. Lan, P. J. Li, J. M. Lin and L. Q. Fan, *Electrochem. Commun.*, 2008, **10**, 1299.
23 H. D. Tran, J. M. D'Arcy, Y. Wang, P. J. Beltramo, V. A. Strong and R. B. Kaner, *J. Mater. Chem.*, 2011, **21**, 3534.
24 Z. Wei and M. Wan, *Adv. Mater.*, 2002, **14**, 1314.
25 L. Zhang and M. Wan, *Adv. Funct. Mater.*, 2003, **13**, 815.
26 Y. Mu, H. Q. Yu, J. C. Zheng, S. J. Zhang and G. P. Sheng, *Chemosphere*, 2004, **54**, 789.
27 J. Stejskal and P. Kratochvíl, *Synth. Met.*, 1993, **61**, 225.
28 A. J. Bard and L. R. Faulkner, in *Electrochemical Methods: Fundamentals and Applications*, John Wiley & Sons, Inc., New York, 2001, ch. 9, pp. 331–367.
29 J. Zhang, X. Li, W. Guo, T. Hreid, J. Hou, H. Su and Z. Yuan, *Electrochim. Acta*, 2011, **56**, 3147.